

Second harmonic heating of sloshing ions in a non-axisymmetric mirror

V. E. Moiseenko¹ and O. Ågren

Uppsala University, Ångström laboratory, SE-751 21 Uppsala, Sweden

¹*Permanent address: Institute of Plasma Physics, National Science Center “Kharkov Institute of Physics and Technology”, 61108 Kharkiv, Ukraine*

Sloshing ions trapped in magnetic mirror are energetic ions that have a certain ratio of perpendicular to parallel velocity. Their concentration increases near the mirror point. The sloshing ions play a substantial role for plasma confinement in mirror traps. Their sustain in a mirror trap could be maintained either by neutral beam injection or radio-frequency (RF) heating. A scenario of light minority sloshing ion heating on the fundamental cyclotron harmonic has been numerically studied in [1]. That study relates to the recently proposed straight field line mirror [2] and sloshing-ions based fusion reactor [3]. In [3], both deuterium and tritium sloshing ions are considered. The problem how to sustain the heavy sloshing ion component with RF heating has not been treated in [1]. In the present paper the second harmonic ion cyclotron heating of the heavy sloshing ion component is considered. The second harmonic ion cyclotron damping of the fast magnetosonic wave (see [4-6]) is caused by the electromagnetic field non-uniformity across the steady magnetic field and the ion thermal motion. It has been experimentally tested in tokamaks [7,8]. Attempts to use the second harmonic ion cyclotron heating have also been made in mirror experiments [9]. As compared with the fundamental harmonic ion cyclotron heating, the second harmonic cyclotron damping is weaker, and the ratio of the damping rates is proportional to $(k_{\perp} \rho_{L\alpha})^2$ which typically is a small number. Here, $\rho_{L\alpha}$ is the ion Larmor radius and α indices the ion component.

The electromagnetic calculations are performed for a reactor-scale straight field line mirror device, schematically shown in Fig. 1. The magnetic field strength of that device is described by the following formula:

$$\mathbf{B}_0 = B_{00} \left[\frac{\mathbf{e}_z}{1 - z^2/c^2} - \mathbf{e}_x \frac{x}{c} \frac{1 + z/c}{(1 - z^2/c^2)^2} + \mathbf{e}_y \frac{y}{c} \frac{1 - z/c}{(1 - z^2/c^2)^2} \right], \quad (1)$$

where c is the half-distance between the left and right poles of the trap. At the poles at $z = \pm c$, the magnetic field strength goes to infinity. In the numerical model, the plasma

diamagnetism is included by adding the finite beta correction to the magnetic field from a prescribed pressure distribution, i.e. $\mathbf{B} = \mathbf{B}_0 \sqrt{1 - \beta}$.

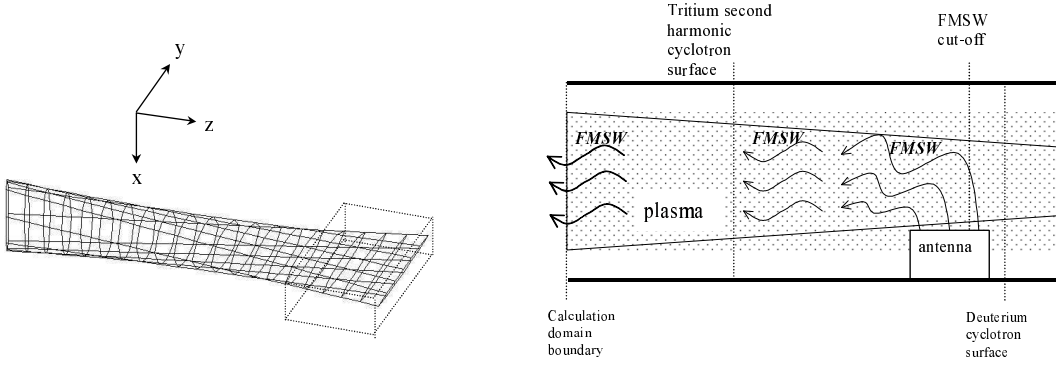


Fig. 1. Straight field line mirror with RF heating computational domain. Fig. 2. Sketch of RF heating scheme.

We consider a reactor-scale device with $c = 50$ m, $a = 150$ cm and $B_{00} = 1.5$ T. Here, a is the plasma radius at the central plane where the magnetic surfaces have a circular cross-section. The trap confines deuterium and tritium sloshing ions in-between the mirror points $z/c = \pm\sqrt{3}/2$. We choose the ends of the trap at $z = \pm 0.9c$ (where the local mirror ratio is 5.3) and consider RF heating at one of the ends, the right one. The computation domain is $z \in (0.82c, 0.9c)$, i.e. 41 m $< z < 45$ m, which covers the second harmonic tritium cyclotron zone. In the model of RF heating of sloshing ions, the above-mentioned segment of the plasma column is surrounded by a rectangular metallic box with one open side at $z = 41$ m and with sizes $L_x = 60$ cm, $L_y = 600$ cm and $L_z = 400$ cm. Because of the presence of sloshing ions, the plasma is non-uniform not only across the plasma column, but also along the magnetic field and there is a plasma density peak near the center of the computational domain.

For second harmonic heating of tritium we consider the antenna system in [1] which is equivalent to a single-strap antenna with the strap aligned along y . We choose the antenna height as $l_x = 10$ cm, the antenna width as $l_z = 20$ cm and the antenna length as $l_y = 500$ cm. The regular position of the antenna with respect to the center of the trap is $z_a = 3388$ cm.

The second harmonic cyclotron resonance is accounted in WKB limit, and the corresponding contribution to the resonant component of the displacement vector can be calculated by the finite Larmor radius expansion [10-12]

$$\delta\mathbf{D} = -\frac{\varepsilon_0}{8} \mathbf{e}_{\parallel} \times \mathbf{e}_{\parallel} \times [\nabla_{\perp} \cdot (\tilde{\varepsilon}_{+2} \nabla_{\perp})] \mathbf{E}_{+} - \frac{\varepsilon_0}{8} i \mathbf{e}_{\parallel} \times [\nabla_{\perp} \cdot (\tilde{\varepsilon}_{+2} \nabla_{\perp})] \mathbf{E}_{+} - \frac{\varepsilon_0}{4} \nabla \tilde{\varepsilon}_{+2} \cdot (\mathbf{e}_{\parallel} \times \nabla) \mathbf{E}_{+}, \quad (2)$$

where $\delta\mathbf{D} = \frac{1}{\sqrt{2}}\mathbf{e}_+\delta D_+$ and $\nabla_{\perp} = \nabla - \mathbf{e}_{\parallel}\mathbf{e}_{\parallel} \cdot \nabla$, $\mathbf{E}_+ = -\frac{1}{2}\mathbf{e}_{\parallel} \times \mathbf{e}_{\parallel} \times \mathbf{E} - \frac{i}{2}\mathbf{e}_{\parallel} \times \mathbf{E}$,

$$\tilde{\varepsilon}_{+2} = \sum_{\alpha} \frac{4\omega_{p\alpha}^2 v_{T\perp\alpha}^2}{\omega |k_{\parallel} v_{T\parallel\alpha}| \omega_{c\alpha}^2} \left[F(\beta_{2\alpha}) - \frac{i\sqrt{\pi}}{2} \exp(-\beta_{2\alpha}^2) \right] \left[1 + (1 - 2\omega_{c\alpha}/\omega)(v_{T\perp\alpha}^2/v_{T\parallel\alpha}^2 - 1) \right], \quad (3)$$

F is the Dawson integral and $\beta_{2\alpha} = (\omega - 2\omega_{c\alpha})/|k_{\parallel} v_{T\parallel\alpha}|$. The advantage of the vector representation (2) is the absence of coordinate-dependent vectors or matrices.

With the expression (2) the power deposition is:

$$p_{+2} = -\frac{\omega\varepsilon_0}{8} \text{Im} \tilde{\varepsilon}_{+2} \nabla_{\perp} \mathbf{E}_+^* : \nabla_{\perp} \mathbf{E}_+ + \frac{\omega\varepsilon_0}{8} \text{Re} \left\{ \mathbf{E}_+^* \cdot \left[\nabla_{\perp} \tilde{\varepsilon}_{+2} \cdot (\mathbf{e}_{\parallel} \times \nabla) \right] \mathbf{E}_+ \right\}, \quad (4)$$

where double dot means double scalar product, first over indices of the electric field and second over indices of the nabla operator. The first term corresponds to the power deposition in uniform plasma, while the second term is a result of non-uniformity. The energy kinetic flux term coincides with that of a uniform plasma:

$$\Pi_{+2} = \frac{\omega\varepsilon_0}{8} \mathbf{E}_+^* \cdot \text{Re} \tilde{\varepsilon}_{+2} \nabla_{\perp} \mathbf{E}_+, \quad (5)$$

where the scalar product operator relates to the electric field vectors.

In the numerical calculations, the following set of parameters is chosen: Plasma density (in its maximum) is $n_{p0} = 5 \cdot 10^{14} \text{ cm}^{-3}$, heating frequency is $\omega = 2.9 \cdot 10^8 \text{ s}^{-1}$, deuterium and tritium parallel and perpendicular thermal velocities at the z -axis are $v_{T\parallel D} = v_{T\parallel T} = 5 \cdot 10^5 \text{ m/s}$ and $v_{T\perp D} = v_{T\perp T} = 1.35 \cdot 10^6 \text{ m/s}$, the deuterium concentration is $C_D = 0.4$.

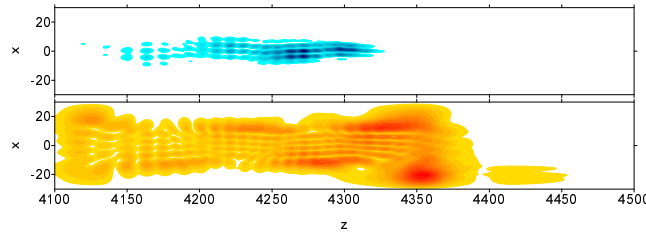


Fig. 3 Lower figure is the electric field module at the cross-section $y = 0$; yellow marks the minimum value, red - maximum. Upper figure is the second harmonic part of the power density projected on the plane $y = 0$, i.e.

$$\bar{p}_{+2} = \int_{-L_y/2}^{L_y/2} p_{+2} dy, \text{ where } L_y \text{ is the plasma size in the } y$$

direction. Dark blue color corresponds to maximum power density.

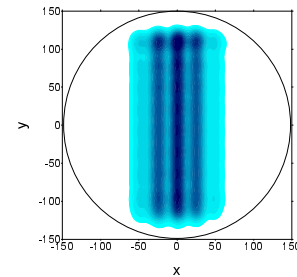


Fig 4. Distribution of RF power deposition

$$\tilde{p}_{+2} = \int_{-L_L}^{L_R} p_{+2} dl \text{ projected on the plane } z = 0.$$

Dark blue color corresponds to maximum power density.

Some results of calculations performed with the numerical model [1] improved by account of (2) in Maxwell's equations are presented in Figs. 3 and 4. Fig 3. shows that the fast magnetosonic wave propagates to lower magnetic field with some gradual decrease in amplitude. The slow wave is almost not visible, and its amplitude is small. The power deposition projected to the $y = 0$ plane is broad along z . This is the result of weak damping of the wave and a broad cyclotron zone. The cyclotron zone is broadened owing to weak magnetic field gradient at the second harmonic cyclotron resonance location. This appears as a result of the influence of sloshing ion pressure on the steady magnetic field.

The power deposition projected along magnetic field lines on the plane $z = 0$ (Fig.4) is core. Its quadratic shape reflects the assumption of plasma uniformity along y . Some shift along y occurs owing to plasma gyrotropy and the asymmetrical antenna placement with respect to the $x = 0$ plane.

Conclusions

The numerical model used in [1] for the calculations of minority heating has been improved with account of the finite Larmor radius corrections to the dielectric tensor. Using it the scenario of second harmonic heavy ion heating has been examined. In the scenario chosen, the regime of global resonance overlapping is achieved that provides good heating performance. The power deposition is core. The amount of deposited power does not depend sensitively on the parameters of the discharge. However, the problem of heating of low-beta plasma within this scenario is still actual.

For RF heating with this scheme, basically a single strap antenna is used, the same as in [1]. The antenna performance is noticeably higher than for minority heating. The scenario studied seems prospective for practical use.

References

1. V.E. Moiseenko, O.Ågren, Phys. Plasmas **12**, ID 102504 (2005).
2. O.Ågren, N. Savenko, Phys. of Plasmas **11**, 5041 (2004).
3. O.Ågren, N. Savenko, Phys of Plasmas **12**, ID 022506 (2005).
4. K.N.Stepanov, ZhETPh **38**, 265 (1960) (in Russian).
5. T.H. Stix, Nuclear Fusion **15**, 737 (1975).
6. F.W. Perkins, Nuclear Fusion **17**, 1197 (1977).
7. J.R. Wilson, C.E. Bush, D. Darrow et al, Phys. Rev. Lett. **75**, 842 (1995).
8. D.F.H. Start, J. Jacquinet, V. Bergeauda et al., Nuclear Fusion **39**, 321 (1999).
9. Y. Yasaka, A. Maruyama, N. Takano, Trans. Fus. Science and Tech. **43**, 44 (2003).
10. S.V.Kasilov, Yu.N.Ledovskoj, V.E.Moiseenko, V.V.Pilipenko, K.N.Stepanov, Physica Scripta **45**, 373 (1992).
11. S.V.Kasilov, A.I.Pyatak, K.N. Stepanov, "Nonlocal theory of cyclotron and Cerenkov absorption in nonuniformly magnetized plasma" Chapter 7, In *Reviews of Plasma Physics* (ed. B. B. Kadomtsev) Vol. 20 (1997). Consultants Bureau, p. 61.
12. M. Brambilla, Plasma Phys. Control. Fusion **31**, 723 (1989).